

ANALYSIS OF HELIUM PURGE FLOW IN A SOLID BREEDER BLANKET *

K. FUJIMURA **, A.R. RAFFRAY and M.A. ABDU

*Mechanical, Aerospace and Nuclear Engineering Department, University of California, Los Angeles,
Los Angeles, CA 90024-1597, USA*

A numerical analysis of the purge flow in sphere-pac solid breeder has been carried out using the modified Darcy equations. The results show that: (1) the tritium accumulation in the purge and permeation through the wall is not a concern. (2) pressure drop expressions for fully developed flow are applicable in evaluating the pressure drop in a developing flow regime because of the very short entry length and (3) the pressure drop for low porosity (~ 20%) and high flow rate considered in conceptual reactor designs can be unacceptably high.

1. Introduction

A separate helium purge is desirable in both water-cooled and helium-cooled solid breeder blanket designs. For the water-cooled case, the idea is to avoid contamination of the coolant with tritium. In the helium-cooled case, use of the main flow to purge tritium also would cause a very large pressure drop and pumping power requirements and part of the heat removed by the coolant would be inefficiently lost in the tritium processing system. Operation at high pressure could also compromise the physical integrity of the breeder. A separate helium purge system can resolve these difficulties and also would minimize tritium in the main stream going to the heat exchanger and therefore minimize tritium release to the environment. Consequently, a separate helium purge system is generally assumed for tritium recovery in solid breeder blanket designs. The helium purge is in direct contact with the solid breeder and transports all the tritium bred in the blanket. Thus, the helium purge has a very large impact on the design, performance, complexity, reliability and safety of the blanket.

This paper addresses some of the thermal-hydraulic issues of a helium purge flowing through a sphere-pac solid breeder bed. Of particular importance is the developing velocity profile of the gas purge and the pressure

drop as a function of porosity. The velocity profile gives information about the boundary layer thickness and regions of stagnation or recirculation, both leading to tritium accumulation and hence higher tritium inventory and potential for tritium permeation through the clad. For a solid breeder plate design, the analysis of the velocity profile can also indicate whether there is any penalty associated with simplifying the helium purge inlet and outlet by locating them at the back of the plate instead of at each end of the plate.

2. Configuration and equations

A rectangular geometry is considered here based on the desire to analyze the plate design of the BCSS helium-cooled solid breeder blanket [1]. This design can be simplified by positioning the helium inlet and outlet at the back of the plate, and hence eliminating the need for a plenum at each end of the plate. Note, however, that the conclusions obtained in this analysis would also apply to other geometries.

The basic equations for steady state fluid motion in a porous media are the continuity and modified Darcy equations: [2]

$$\nabla \cdot u = 0, \quad (1)$$

$$0 = -\nabla p - (\mu/K)u - \mu_{eff} \nabla^2 u - (\rho C/\sqrt{K})|u|u, \quad (2)$$

where u is the velocity vector, p is the pressure, μ is the dynamic viscosity of the fluid, K is the porous medium permeability, C is the inertia coefficient, ρ is

* Work performed under US Department of Energy Grant No. DE-FG03-86ER52123.

** On leave from Japan Atomic Energy Research Institute, Tokai-mura, Ibaraki, 319-11.

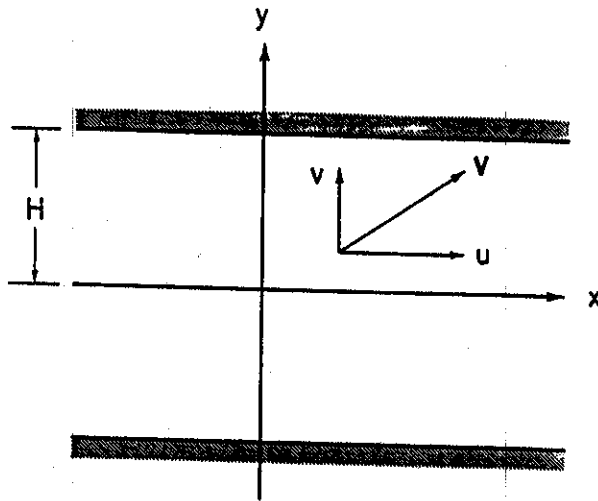


Fig. 1. Rectangular channel configuration for which the porous flow equations are solved.

the density of the fluid and μ_{eff} is the effective dynamics viscosity of the fluid in the porous region.

The last three terms in eq. (2) account for the Darcy (porous media), Brinkman (friction caused by macroscopic shear) and Forchheimer (flow inertia) effects, respectively. For uniformly packed spheres of diameter, d , the coefficients K , C and μ_{eff} can be evaluated as $K = d^2 \phi^3 / [175(1 - \phi)^2]$, $C = (1.75 / \sqrt{175}) \phi^{-3/2}$ and $\mu_{\text{eff}} = \mu$, where ϕ is the porosity defined by the ratio of the purge flow volume to the entire channel volume [2].

For the 2-D case shown in fig. 1, the stream function, $\Psi(x, y)$, can be introduced to eliminate the pressure terms and, after non-dimensionalization, eqs. (1) and (2) become

$$\begin{aligned} \text{Re}^{-1} [\Delta - \text{Da} \Delta^2] \psi \\ = -C \text{Da}^{1/2} \left[|v| \Delta \psi + \frac{\partial \psi}{\partial x} \frac{\partial |v|}{\partial x} + \frac{\partial \psi}{\partial y} \frac{\partial |v|}{\partial y} \right] \end{aligned} \quad (3)$$

where v is the non-dimensional velocity vector (normalized by average velocity, U), Re is the Reynolds number defined by UH/ν , Da is the Darcy number defined by K/H^2 , H is the channel half-width and $\Delta = \partial^2/\partial x^2 + \partial^2/\partial y^2$.

A computer program was written to solve the above equation using an expansion method in Chebyshev polynomials subject to the given boundary conditions. The stream function ψ was expanded as

$$\psi(x, y) = \sum_{m=0}^{\infty} \sum_{n=0}^{\infty} a_{mn} T_m(x) T_n(y) \quad (4)$$

where T_m and T_n are the Chebyshev polynomials of

the m th and n th degree, respectively. The number of terms of the Chebyshev polynomial included in the expansion was truncated at some finite value, N (≤ 30), because of the limitation of the computer memory size. The collocation method was utilized in order to reduce eq. (3) to $(N+1) \times (N+1)$ nonlinear algebraic equations for the expansion coefficients a_{mn} and the Newton method was used to solve these equations for a_{mn} .

3. Fully-developed flow

Eq. (3) was first solved to obtain the fully-developed velocity profile when the stream function varies with y only and a non-slip boundary condition at the solid wall is imposed. The velocity profile, $u(y)$, as a function of the distance, y , from the center of the channel is shown in fig. 2 for different porosities ϕ and for $\text{Re} = 1$. The effect of adding even a small percentage of spheres is quite dramatic as the velocity profile is substantially flattened as shown by the difference between the $\phi = 1.0$ (normal flow) and $\phi = 0.95$ cases.

The results from fig. 2 were used to calculate the boundary layer thickness as a function of porosity for different Re . The objective was to examine whether tritium accumulation in the boundary layer could become a problem by enhancing tritium permeation through the structural wall to the main coolant. Fig. 3

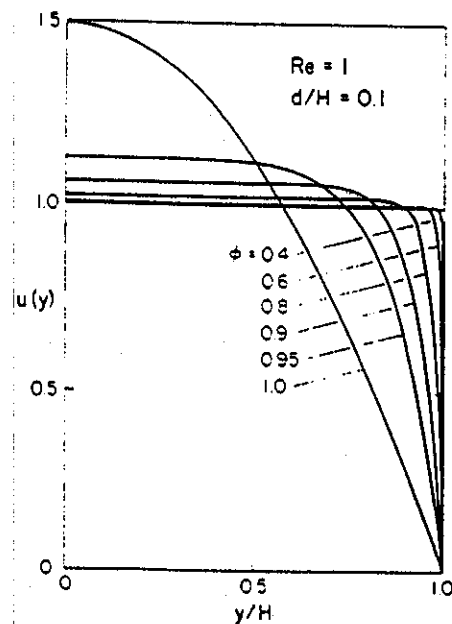


Fig. 2. Velocity profile as a function of distance from the center line for different porosities.

Table 1

Comparison of time constants for tritium diffusion^a across boundary layer to those for tritium diffusion through a solid breeder grain and permeation through a stainless steel wall ($t_w = 0.1$ cm, $\delta = 0.01$ and the channel half-width = 1 cm)

Solid breeder	T (K)	D_{He} (m ² /s)	D_g (m ² /s)	D_p (m ² /s)	r_g (μ m)	t_c (s)	t_g (s)	t_p (s)
Li ₂ O	673	2.1×10^{-5}	1.5×10^{-13}	2.4×10^{-11}	2.0	4.7×10^{-4}	26.7	4.2×10^4
	1073	4.1×10^{-5}	2.3×10^{-11}	8.9×10^{-10}		2.4×10^{-4}	0.17	1.1×10^3
LiAlO ₂	673	2.1×10^{-5}	3.7×10^{-21}	2.4×10^{-11}	0.2	4.7×10^{-4}	1.1×10^7	4.2×10^4
	1273	5.3×10^{-5}	3.2×10^{-16}	2.3×10^{-9}		1.9×10^{-4}	125.0	435.0
Li ₄ SiO ₄	623	1.8×10^{-5}	9.0×10^{-17}	1.1×10^{-11}	2.0	5.6×10^{-4}	4.4×10^4	9.1×10^4
	1123	4.4×10^{-5}	2.2×10^{-14}	1.2×10^{-9}		2.3×10^{-4}	181.8	833.3

^a Diffusion constants used are given by the following expressions:

- D_{He} (m²/s) = $1.17 \times 10^{-9} T^{3/2}$ for 0.1 MPa pressure. [3].
- D_g (Li₂O) = $1.17 \times 10^{-7} \exp(-9.1 \times 10^3/T)$. [4].
- D_g (LiAlO₂) = $1.1 \times 10^{-10} \exp(-1.6 \times 10^4/T)$. [4].
- D_g (Li₄SiO₄) = $2.1 \times 10^{-11} \exp(-7.7 \times 10^3/T)$. [4].
- D_p (stainless steel) = $3.8 \times 10^{-7} \exp(-6.5 \times 10^3/T)$. [5].

shows that the boundary layer thickness, δ , normalized to the channel half-width, H , increases markedly with increasing porosity but is only slightly affected by the choice of Re in particular in the range of 0.1–100. The criterion used to calculate δ was for the velocity to be 99% of the center line velocity.

The time constant for tritium diffusion from the boundary layer to the core flow, $t_c = \delta^2/D_{He}$, was

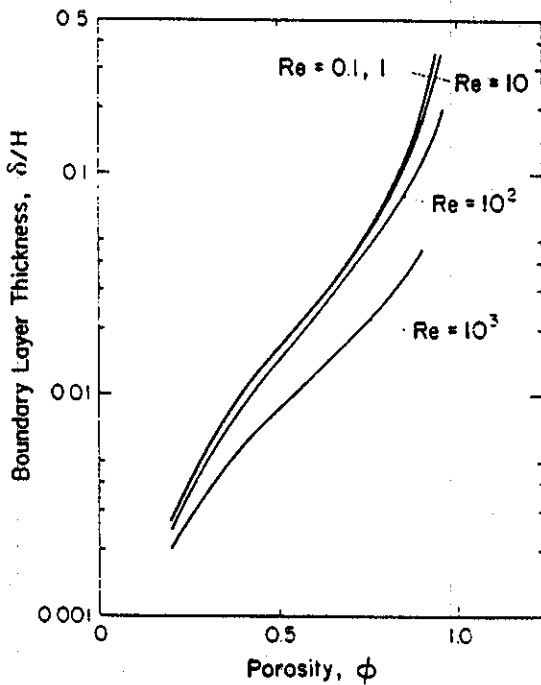


Fig. 3. Boundary layer thickness as a function of porosity for different values of the Reynolds numbers.

compared to the time constant for tritium diffusion through a solid breeder grain, $t_g = r_g^2/D_g$, and to the time constant for tritium permeation through the wall, $t_p = \delta_w^2/D_p$.

D_{He} , D_g and D_p are the tritium diffusion coefficients in He, a solid breeder grain and the wall, respectively. r_g is the radius the solid breeder grain and δ_w is the thickness of the wall.

For a stainless steel wall and three different solid breeder material (Li₂O, LiAlO₂ and Li₄SiO₄), t_c , t_g and t_p were calculated at the lowest and highest allowable solid breeder operating temperatures which are determined from tritium inventory considerations. Expressions for the diffusion coefficients, D_{He} , D_g and D_p were obtained from refs. [3], [4] and [5] respectively. The results are shown in table 1 for $\delta = 0.01$ corresponding to a porosity of about 40%. Since the porosity of solid breeder sphere-pac configuration will be lower than that (almost 20%), the results are conservative. Clearly, the time constant for tritium diffusion through the boundary layer to the core flow is orders of magnitude shorter than the time constants for both tritium permeation through the wall and tritium diffusion through the solid breeder grain. This indicates that any tritium in the boundary layer will diffuse to the core flow much faster than tritium diffusing out of the grain, and that, consequently, tritium accumulation in the boundary layer will not occur. Even if tritium accumulation were present, the results indicate that tritium will diffuse to the core flow much faster than through the wall and that permeation is orders of magnitude slower than convection to and transport by the helium purge.

4. Developing flow

The expansion method in Chebyshev polynomials used to solve eq. (3) in 2-D was first validated by successfully solving for the well-known cavity flow problem for normal hydrodynamic flow. The method was then applied to the solution of porous flow along a solid breeder plate. The objectives were to observe the streamlines inside the plate and to find out how they are affected by the location of the inlet and outlet, and also to examine the effect of porosity on the entry length. This would also be important in determining whether the pressure drop correlation for fully developed flow in a porous media can be adequately used to estimate the pressure drop for developing flow.

Figs. 4 and 5 show examples of the streamlines inside a typical plate for two different inlet/outlet configurations with slug flow assumed at the inlet and outlet. The porosity is quite high (0.95) since solutions for lower porosity are very hard to obtain due to the length of computational time. However, results for higher porosities, such as those shown in these two figures, illustrate the dampening effect of the presence of solid particles in the flow. The flow tends to sweep the whole plate and there is no vortical structure or stagnation region where tritium accumulation could occur.

Although the results shown are for $Re = 1$, the conclusions can be extended to the solid breeder plate case for Re of about 10-100 since the porosity in this case

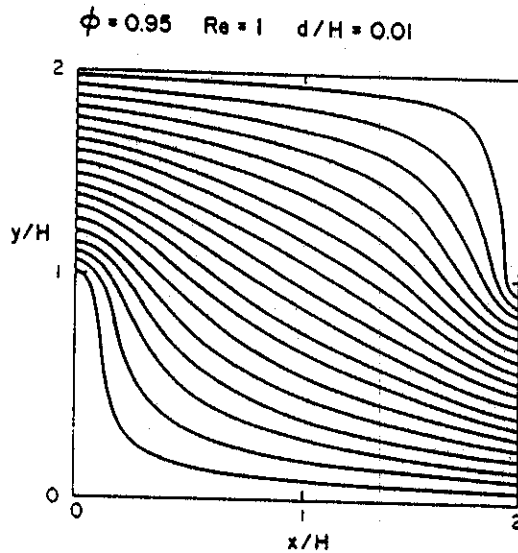


Fig. 4. Streamlines for helium purge flow in porous solid breeder plate with inlet in top half of plate and outlet in bottom half of plate.

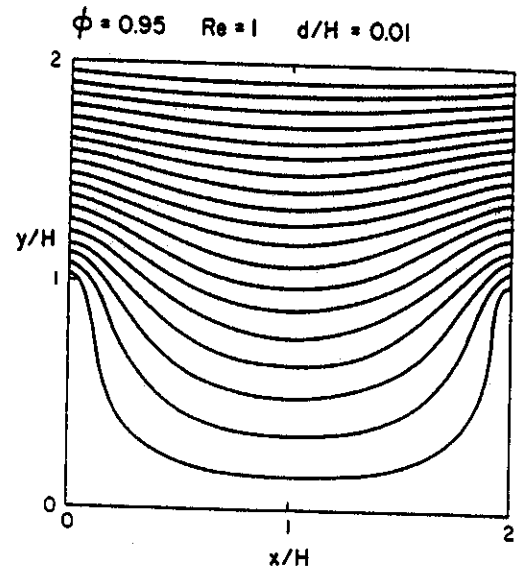


Fig. 5. Streamlines for helium purge flow in porous solid breeder plate with both inlet and outlet in top half of plate.

will be low (about 20-30%). The indications are that the inlet and outlet of the purge flow could be positioned at each end of the back of the plate and the purge flow would still sweep the whole solid breeder area.

Fig. 6 shows the developing flow profile for flow in a porous channel with porosities of 0.95 and 0.85. The inlet velocity profile is assumed parabolic and it can be

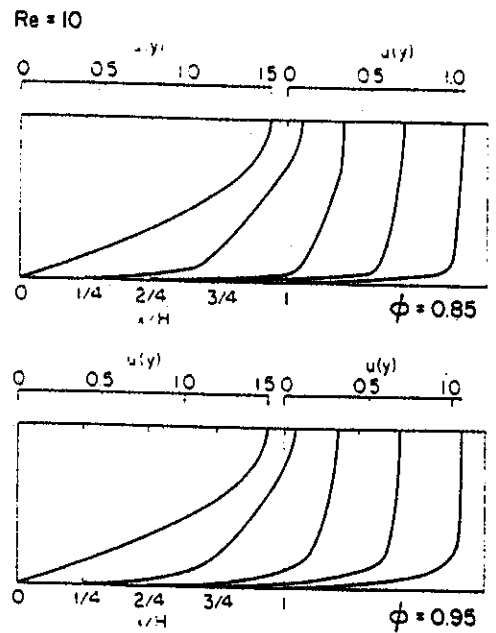


Fig. 6. Developing velocity profiles for porous flow with porosities of 0.85 and 0.95.

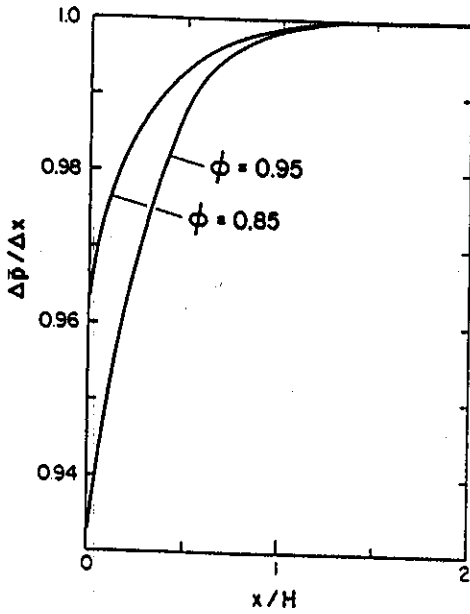


Fig. 7. Pressure gradient as a function of length along the channel for porosities of 0.9 and 0.95.

$$\frac{\Delta \bar{p}}{\Delta x} = \left[\frac{1}{2H} \int_{-H}^H \frac{\partial p}{\partial x} dy \right] / (\partial p / \partial x) |_{x \rightarrow \infty}$$

seen that within about one channel half-width, the flow becomes fully developed. Porosity again flattens the velocity profile very quickly and it is expected that fully developed flow will occur even sooner for lower porosi-

ties. Fig. 7 shows the corresponding pressure gradient normalized to the fully developed pressure gradient for these two cases. This figure shows that the pressure drop correlation obtained for the fully developed flow regime is applicable to evaluate the pressure drop for an inlet flow problem for channel lengths greater than about the channel width (or shorter for lower porosities).

Based on the above conclusion, the pressure drop expression for fully developed flow was used to calculate the pressure drop in a solid breeder plate as a function of porosity. Non-dimensionalization of eq. (2) and elimination of non-dominant terms yields the expression: $dp/dx = Re^{-1} Da^{-1} u$, where $Da^{-1} = (H/d)^2 175(1-\phi)^2 / \phi^3$. This equation is basically the same as the empirical correlation recommended in ref. [6].

Fig. 8 shows the variation of pressure drop with porosity for different Re and d/H for a solid breeder plate. The required pumping power for a total purge flow rate of $3 \text{ m}^3/\text{s}$, typical of reactor conditions, is also shown and can be seen to be quite small for particle to channel diameter ratios greater than 0.1 and porosities greater than 0.2. A more binding constraint for porosities of about 0.2, as proposed in past designs [1], is the pressure drop which, in the case of a Re of 10, would require the purge flow pressure to be about 1 MPa. A higher Re would decrease the tritium partial pressure in the purge gas but would increase the pressure drop by about a factor of 10. Such high pressure drops are

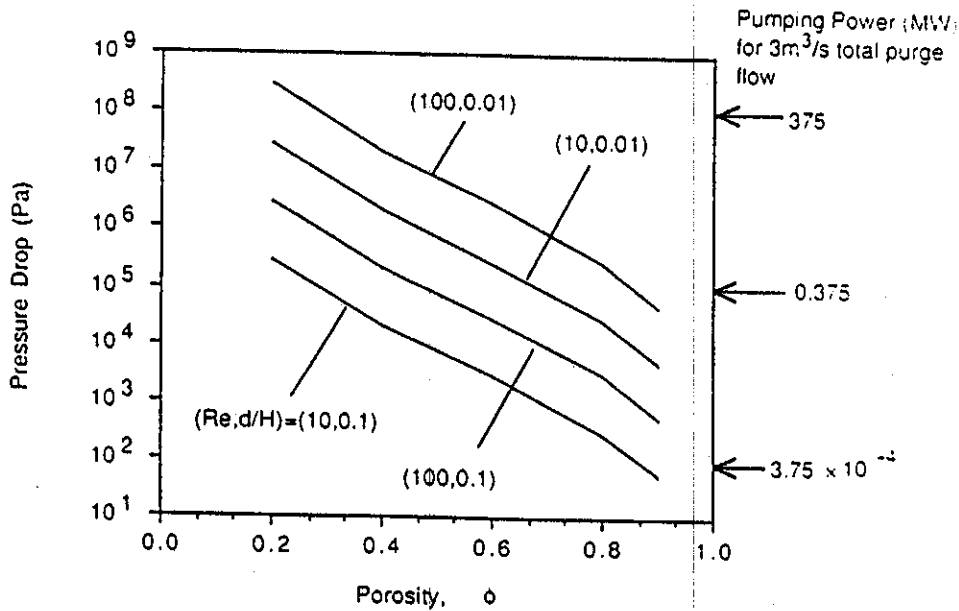


Fig. 8. Purge flow pressure drop as a function of porosity for two different values of Reynolds number Re and particle diameter to channel width ratio (d/H).

unacceptable not only because of the pumping power requirements but also because of the effect of high pressures on the physical integrity of the solid breeder material. These observations are important and must be considered in the future in solid breeder blanket design and analysis. Consideration should be given to the choice of the solid breeder sphere and channel sizes, and to helium purge flow rate which would yield acceptable values for the pressure drop, pumping power and tritium partial pressure. The results also indicate that use of the main coolant to purge tritium at higher velocities and Reynolds number would lead to unacceptable pressure drops and pumping power requirements.

5. Concluding remarks

Analysis of the purge flow in sphere-pac solid breeder blanket design has shown that: (1) Fully developed boundary layer thickness for porous flow is small enough that any tritium present in the boundary layer would diffuse back to the core flow much faster than it would permeate through the wall and much faster than tritium generated in the solid breeder would diffuse through the breeder grain. Thus, tritium accumulation in the boundary layer and permeation through the wall due to the slowly moving boundary layer is not a concern. (2) For Re of about 1–100, porous flow tends to sweep the whole area of flow for different inlet/outlet conditions and does not show any vortical structure or stagnation region which would lead to tritium accumulation. This purge flow characteristic can be used advantageously for a plate design by positioning the inlet and outlet of the purge flow at each end of the back of the plate, thereby simplifying the design. (3) As the entry length for porous flow is short (of the order of one

channel width), pressure drop expressions for fully developed flow can be used to adequately calculate the pressure drop for entry flow. (4) Analysis of the purge flow should be carefully carried out for solid breeder blanket designs because the pressure drop can be unacceptably high for the type of low porosity ($\sim 20\%$) considered in reactor designs. A high pressure in the helium purge would negate one of the advantages of a separate helium purge, which is to minimize the pressure of the fluid in direct contact with the solid breeder. (5) Extrapolation of the results indicates that using the main flow to purge tritium at higher velocities would be unacceptable for the type of porosities proposed for blanket designs (30% or less). The pressure drop and pumping power requirements would be much too large.

References

- [1] D. Smith et al., Blanket comparison and selection study, Final Report, (Argonne National Laboratory, Illinois, 1984) ANL/FPP-84-1.
- [2] D. Poulikakos, Buoyancy-driven convection in a horizontal fluid layer extending over a porous substrate, *Phys. Fluids* 29 (1986) 3949–3957.
- [3] W.M. Rohsenow and H.Y. Choi, Heat, mass and momentum transfer, (Prentice-Hall, New Jersey, 1981) pp. 382–383.
- [4] M.A. Abdou et al., Modeling, analysis and experiments for fusion nuclear technology (FNT Progress Report: Modeling & FINESSE), (University of California, Los Angeles, 1987) PPG-1021, UCLA-ENG-86-44, FNT-17.
- [5] B.L. Doyle and D.K. Brice, Steady state hydrogen transport in solids exposed to fusion reactor plasmas, part II applications of theory, *J. Nucl. Matter.* 122–123 (1984) 1527–1530.
- [6] J.H. Perry, ed., Handbook of Chemical Engineering, (McGraw-Hill, New York, 1950) pp. 393–394.